

Self-Imitated Diffusion Policy for Efficient and Robust Visual Navigation

Runhua Zhang^{1,2*}, Junyi Hou^{1,2*}, Changxu Cheng^{1†},
 Qiyi Chen¹, Tao Wang¹, Wuyue Zhao¹
¹Uni-Ubi ²Zhejiang University

Abstract—Diffusion policies (DP) have demonstrated significant potential in visual navigation by capturing diverse multi-modal trajectory distributions. However, standard imitation learning (IL), which most DP methods rely on for training, often inherits sub-optimality and redundancy from expert demonstrations, thereby necessitating a computationally intensive “generate-then-filter” pipeline that relies on auxiliary selectors during inference. To address these challenges, we propose *Self-Imitated Diffusion Policy (SIDP)*, a novel framework that learns improved planning by selectively imitating a set of trajectories sampled from itself. Specifically, SIDP introduces a reward-guided self-imitation mechanism that encourages the policy to consistently produce high-quality trajectories efficiently, rather than outputs of inconsistent quality, thereby reducing reliance on extensive sampling and post-filtering. During training, we employ a reward-driven curriculum learning paradigm to mitigate inefficient data utility, and goal-agnostic exploration for trajectory augmentation to improve planning robustness. Extensive evaluations on a comprehensive simulation benchmark show that SIDP significantly outperforms previous methods, with real-world experiments confirming its effectiveness across multiple robotic platforms. On Jetson Orin Nano, SIDP delivers a $2.5\times$ faster inference than the baseline NavDP, *i.e.*, 110ms VS 273ms, enabling efficient real-time deployment.

I. INTRODUCTION

Diffusion-based path planning has recently emerged as a powerful paradigm for visual navigation [1], [2]. By modeling entire trajectories through iterative denoising, these policies ensure spatiotemporal consistency compared to sequential action prediction [3]. The generative nature of diffusion allows the policy to capture multi-modal trajectory distributions, making it well suited to complex environments with multiple feasible routes to a goal.

A common strategy to train diffusion policies is imitation learning (IL) using expert demonstrations. However, IL introduces two critical bottlenecks. First, robustness is compromised by the limited coverage of expert datasets, causing policies to struggle under distributional shifts and fail in novel scenarios [4], [5]. Second, inference efficiency is affected. Standard IL attempts to imitate all given trajectories, including a diverse set of suboptimal ones, which leads to increased sampling variance and heterogeneous trajectory quality. Consequently, inference typically relies on a “generate-then-filter” pipeline with auxiliary trajectory selectors [1], [6]–[8] to select among numerous sampled candidates, which leads to increased latency, especially on resource-constrained devices. These challenges for classic imitation-based diffusion policy are illustrated in Fig. 1(a).

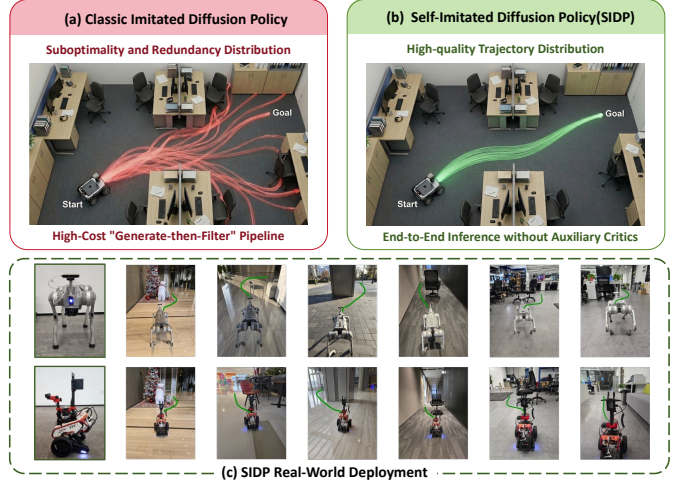


Fig. 1: Comparison between imitation and self-imitation based diffusion policy. (a) The classic imitation-based diffusion policy tends to generate trajectories with high variability, including unsafe, non-shortest or goal-unreachable routes, therefore relies on extensive sampling with post-filtering to obtain a final plan. (b) SIDP achieves distribution concentration via reward-guided self-imitation, enabling robust and efficient path planning without auxiliary selectors. (c) Validation across two robot platforms in real-world environments.

In this work, we propose the **Self-Imitated Diffusion Policy** (SIDP), a framework designed for efficient and robust path planning in visual navigation.

SIDP employs a reward-guided self-imitation scheme [9], in which target trajectories are self-generated by the policy rather than sourced from external demonstrations. By reweighting these trajectories based on their rewards, the framework prioritizes learning from high-quality experiences. This training design facilitates iterative policy refinement by leveraging diverse navigation data and environmental feedback, thereby empowering the policy to develop **robust** behaviors that generalize beyond the inherent biases of fixed expert datasets. Beyond improving generalization, SIDP circumvents the complexity of RL-tuned diffusion [10], [11] by eliminating the need for backpropagation through the entire sequence of denoising steps, a practice known as Backpropagation Through Time (BPTT) that is often computationally prohibitive and numerically unstable [12]. By reformulating this challenging optimization into an iterative imitation learning objective, SIDP achieves stable policy gradients efficiently. Furthermore,

*Co-first authors. †Corresponding author: cx0127@gmail.com

this self-imitation paradigm fundamentally enhances navigation **efficiency** by fostering distributional concentration. Our policy preserves inter-modal diversity and promoting intra-modal convergence since suboptimal and redundant trajectories are progressively pruned during self-imitation learning. This inherent refinement obviates the need for dense sampling and post-filtering, thus eliminating the reliance on an external selector and resulting in a more streamlined, end-to-end inference process. Besides, deterministic sampling with fewer denoising steps [13] is thus made feasible, which can further speed up the inference.

Under the SIDP framework, we devise two complementary learning strategies to augment the training process. First, we incorporate goal-agnostic exploration to enable autonomous navigation capabilities and diversify the trajectory pool, which also provides a critical regularization effect for point-goal navigation. Second, a reward-driven curriculum learning scheme is employed to prioritize scenarios with high learning potential, effectively addressing the issue of inefficient data utility by dynamically selecting the most constructive training samples throughout the training process.

Through extensive experiments, SIDP achieves state-of-the-art performance on the InternVLA-N1 S1 Benchmark [1], outperforming existing methods in both Success Rate (SR) and Success weighted by Path Length (SPL). While the recent baseline method exhibits a significant performance degradation when transitioning from synthetic training scenes to complex, high-fidelity test environments, SIDP effectively mitigates this distribution shift. Specifically, SIDP surpasses NavDP by approximately 10 points on the InternScene-Commercial setting, underscoring its superior generalization capabilities and robustness in unseen, unstructured environments. Furthermore, SIDP boosts the inference efficiency of the baseline to $2.5\times$ on the Jetson Orin Nano without compromising navigation performance, reducing the latency from 273 ms to 110 ms. Successful deployment across two distinct robotic platforms confirms that SIDP provides a practical solution for real-world visual navigation.

The key contributions are summarized as follows:

- We propose a Self-Imitated Diffusion Policy that enhances robustness through high-quality self-generated experiences. By fostering distributional concentration, SIDP eliminates the need for dense sampling and post-filtering, streamlining the planning process.
- We introduce goal-agnostic exploration and reward-driven curriculum learning, which effectively diversifies trajectory pool and mitigates inefficient data utility, thus regularizing point-goal navigation and promoting convergence.
- SIDP achieves state-of-the-art performance on high-fidelity benchmarks in SR and SPL. Besides, it achieves a $2.5\times$ inference speedup on the edge devices, Jetson Orin Nano, demonstrating its practicality for real-world robotics.

II. RELATED WORK

A. Path Planning in Visual Navigation

Path planning in visual navigation can be categorized into mapping-based and learning-based approaches. Mapping-

based methods [14], [15] rely on visual Simultaneous Localization And Mapping(vSLAM) for map construction and pose estimation, followed by graph-search or sampling-based planners such as Dijkstra, A*, or RRT* to compute feasible paths. While effective in structured static environments, these methods are constrained by the need for precise mapping and heuristic planning algorithms, reducing robustness in dynamic or perceptually degraded scenarios.

In contrast, learning-based approaches avoid explicit mapping by either training policies in simulation or directly imitating expert demonstrations. Previous reinforcement learning (RL) methods [16]–[18] exploit reward signals derived from environmental priors to train navigation policies, but incur high computational cost and transfer poorly to real-world domains. Imitation learning (IL) offers better data efficiency [19]–[24]. However, IL-based planners are constrained by the scarcity and fidelity of expert demonstrations, frequently suffering from distribution shift. Moreover, they lack robust mechanisms to suppress compounding errors, which leads to drift during long-horizon navigation. Interactive IL frameworks [25], [26] mitigate such issues by iteratively refining expert datasets.

B. Planning Methods Based on Diffusion Policy

Diffusion models have recently gained attention in sequential decision-making for their ability to capture multimodal distributions via iterative denoising compared to other autoregressive [19]–[22] and latent-variable models [23], [24]. Diffuser [3] reformulates reinforcement learning as conditional trajectory generation, while Decision Diffuser [27] extends this by conditioning on returns and constraints. Later works further explore extensions to long-horizon tasks through hierarchical or compositional formulations [28], [29].

These advances have motivated the application of diffusion policies to path planning. NoMaD [2] directly generate trajectories from observations and integrate goal masking for goal-conditioned and undirected exploration. NavDP [1] leverages privileged information in simulation for path planning in indoor scenes. Some works integrate diffusion into classical planning pipelines to improve collision avoidance and planning efficiency [30], [31], or employ guided sampling strategies to enforce safety and encourage exploration [6], [32]–[36]. These approaches demonstrate that diffusion can flexibly model diverse candidate trajectories while incorporating task-specific constraints or guidance. However, they often require an auxiliary rule-based or learned selector [1], [7], [8] to assess and filter trajectories generated through diffusion sampling, in order to ensure feasibility and safety. Such dependencies increase architectural complexity, posing bottlenecks to both computational efficiency and performance during real-world deployment. These limitations underscore the need for paradigms that intrinsically streamline trajectory generation, enabling robust, end-to-end planning with both theoretical elegance and practical efficiency.

III. METHOD

A. Problem Formulation

We address visual navigation, where an agent generates collision-free optimal trajectories to a specified goal using only

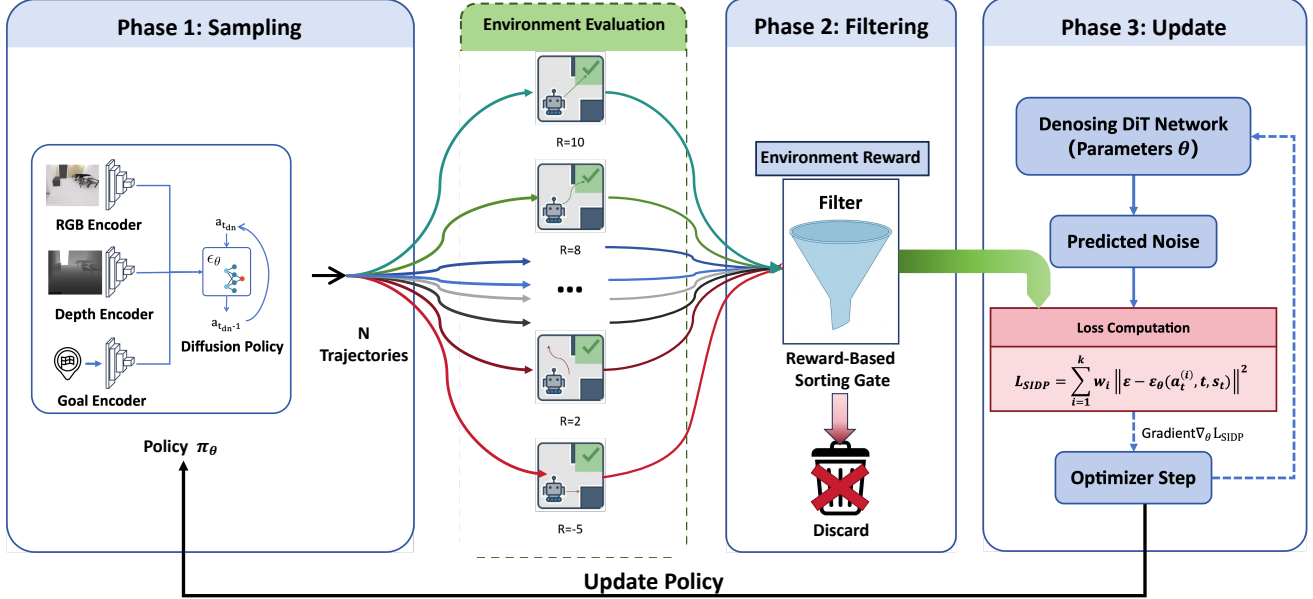


Fig. 2: Overview of the Self-Imitated Diffusion Policy (SIDP). The framework generates candidate trajectories using the current policy π_θ and filters them via a reward-based sorting gate. High-reward samples are then used to compute the weighted denoising loss $\mathcal{L}_{\text{SIDP}}$, updating the policy parameters to iteratively align with the optimal distribution.

egocentric RGB-D observations. The input state is:

$$s_t = (I_t^{\text{RGB}}, I_t^{\text{D}}, g_t) \quad (1)$$

where the RGB image $I_t^{\text{RGB}} \in \mathbb{R}^{H \times W \times 3}$ and depth map $I_t^{\text{D}} \in \mathbb{R}^{H \times W}$ are from the camera observation, and *point goal* $g_t \in \mathbb{R}^3$ are expressed relative to the camera's reference frame. The policy predicts an action sequence of fixed H relative waypoint displacements:

$$a_t = (\Delta p_t^1, \dots, \Delta p_t^H) \in \mathbb{R}^{H \times 3} = \pi_\theta(s_t). \quad (2)$$

To formally evaluate trajectories, we define a quality metric $r(s_t, a_t)$ that rewards safety (collision-free navigation) and efficiency (optimal path toward the goal). The ideal navigation policy π_θ seeks to maximize the expected trajectory quality metric across the state distribution \mathcal{D} :

$$\max_{\theta} \mathbb{E}_{s_t \sim \mathcal{D}, a_t \sim \pi_\theta(\cdot | s_t)} r(s_t, a_t). \quad (3)$$

B. Self-Imitated Diffusion Policy

We solve the problem defined in Eq. (3) from the distribution matching perspective, *i.e.*, to update the policy π_θ to fit a theoretically optimal trajectory distribution $p^*(a|s_t)$. In practice, this is evolved and implemented by a simple yet effective self-imitation process.

1) *Distribution Matching*: Maximizing the expected reward reduces to matching π_θ with the optimal distribution p^* , which is achieved by minimizing the KL-divergence $D_{\text{KL}}(p^* \parallel \pi_\theta)$. This can be further simplified to maximizing the expected log-likelihood under p^* :

$$\begin{aligned} & \arg \min_{\theta} D_{\text{KL}}(p^* \parallel \pi_\theta) \\ &= \arg \min_{\theta} \mathbb{E}_{a \sim p^*} [\log p^*(a|s_t) - \log \pi_\theta(a|s_t)] \\ &= \arg \max_{\theta} \mathbb{E}_{a \sim p^*} [\log \pi_\theta(a|s_t)]. \end{aligned} \quad (4)$$

TABLE I: Reward Components

Component	Formulation
<i>Safety</i>	
Collision	$r_{\text{col}} = -\lambda_{\text{col}} \cdot \mathbb{I}(\text{collision})$
<i>Efficiency</i>	
Step Cost	$r_{\text{step}} = -\lambda_{\text{step}} \cdot (L_{\text{path}}/d_{\text{init}})$
Progress	$r_{\text{prog}} = \lambda_{\text{prog}} \cdot \Delta d_{\text{geo}}$
Docking	$r_{\text{dock}} = \lambda_{\text{dock}} \cdot \psi(d_t) \cdot \mathbb{I}(d_t < \delta_{\text{fine}})$
Total	$r = r_{\text{col}} + r_{\text{step}} + r_{\text{prog}} + r_{\text{dock}}$

Settings: $\lambda_{\text{col}}=10, \lambda_{\text{step}}=0.5, \lambda_{\text{prog}}=5, \lambda_{\text{dock}}=10$.

Definitions: $\mathbb{I}(\cdot)$ is the indicator function. Δd_{geo} is geodesic distance reduction. L_{path} : trajectory length; d_{init}, d_t : start and terminal distances to goal.

Docking: $\psi(d) = \exp(-5(d/d_{\text{init}})^2)$ activates within the fine-tuning region $\delta_{\text{fine}}=0.5$ m.

Since direct sampling from the theoretical target p^* is intractable, we leverage the current policy π_θ as a proposal distribution to generate N candidate actions $\mathcal{A}_t = \{a_t^{(i)}\}_{i=1}^N \sim \pi_\theta(\cdot | s_t)$ via importance sampling (Fig. 2, Phase 1). Thus the objective is converted as:

$$\max_{\theta} \sum_{i=1}^k w(a_t^{(i)}) \log \pi_\theta(a_t^{(i)} | s_t). \quad (5)$$

where $w(a_t^{(i)})$ is the importance weight of the i -th candidate.

2) *Importance Weights*: According to REPS [37], the optimal distribution that maximizes the expected reward, subject to a KL-divergence trust-region constraint relative to the current policy, is analytically given by:

$$p^*(a|s_t) \propto \pi_\theta(a|s_t) \exp \left(\frac{r(s_t, a)}{\tau} \right), \quad (6)$$

where τ is the temperature parameter that controls the constraint strength, π_θ denotes the reference (current) policy. Generally, the importance weights [38] assigned to the candidates are the likelihood ratio $w = p^*/\pi_\theta$. Combining with Eq. (6), we have w relying solely on the trajectory quality $r(s_t, a)$. Our reward setting are detailed in Tab. I.

To mitigate the high variance caused by the exponential nature of Boltzmann distributions, we apply a top- k truncation strategy that retains only the k highest-reward candidates to cover the dominant modes of p^* , as shown in Fig. 2 phase-2. The rewards are normalized to have importance weights:

$$w(a_t^{(i)}) = \frac{\exp(r(s_t, a_t^{(i)})/\tau)}{\sum_{j=1}^k \exp(r(s_t, a_t^{(j)})/\tau)} \quad (7)$$

3) *Self-Imitated Diffusion Policy Loss*: Inspired by the derivation in DDPM [39], maximizing the weighted log-likelihood is reduced to minimizing the reward-weighted denoising loss, which is exactly our SIDP objective:

$$\mathcal{L}_{\text{SIDP}} = \sum_{i=1}^k w(a_t^{(i)}) \mathbb{E}_{t_{dn}, \epsilon} \left[\left\| \epsilon - \epsilon_\theta(a_t^{(i)}, t_{dn}, s_t) \right\|_2^2 \right] \quad (8)$$

where t_{dn} is the diffusion timestep and ϵ is the noise.

At this point, the complete SIDP framework is fully established. Refer to Algorithm 1 for a summary view. By integrating reward-guided self-imitation with the representational power of diffusion models, SIDP forms a coherent pipeline for iterative policy refinement.

Algorithm 1 Self-Imitated Diffusion Policy (SIDP)

```

1: Input: Policy network  $\pi_\theta$ , candidate count  $N$ , truncation
    $k$ , temperature  $\tau$ 
2: Initialize: Environment  $\mathcal{E}$ 
3: while NOT converged do
4:   // Phase 1: Online Sampling
5:   Observe current state  $s_t$  from environment  $\mathcal{E}$ 
6:   Generate  $N$  candidate actions  $\mathcal{A}_t$  using  $\pi_\theta$ .
7:   // Environment: Reward Evaluation
8:   for each candidate action  $a_t^{(i)} \in \mathcal{A}_t$  do
9:     Evaluate action quality:  $R_i = r(s_t, a_t^{(i)})$ 
10:    end for
11:   // Phase 2: Filtering – Importance weighting
12:   Select top- $k$  actions with highest  $R_i$ :  $\mathcal{A}_t^{\text{top-}k}$ 
13:   Compute normalized importance weights (Eq. 7).
14:   // Phase 3: Parameter Update (On-Policy)
15:   Sample diffusion step  $t$  and noise  $\epsilon \sim \mathcal{N}(0, I)$ 
16:   Compute weighted denoising loss (refer to Eq. 8).
17:   Update policy parameters using  $\nabla_\theta \mathcal{L}_{\text{SIDP}}$ 
18: end while
19: Output: Optimized policy  $\pi_\theta$ 

```

C. Complementary Learning Strategies

To further augment the capabilities of the SIDP framework, we devise two synergistic strategies: goal-agnostic exploration and reward-driven curriculum learning.

1) *Goal-agnostic Exploration*: We augment the training process with an extra *goal-agnostic* setting, to activate the exploration ability [2] and regularize the point-goal navigation learning. At each environment reset, we first sample auxiliary goal points following a uniform angular and distance distribution within the range of $-60 \sim 60^\circ$ and $3 \sim 5$ m. Then feasible secure paths towards these goals are generated by the current policy π_θ .

During the training forward pass, the point goal g_t in the input state Eq. (1) is replaced with a special goal-agnostic embedding, while the importance weights in Eq. (5) are set to be uniform. This strategy facilitates goal-agnostic exploration by decoupling policy behaviors from specific objectives. Meanwhile, the sampled trajectories exhibit increased diversity, preventing the policy from overfitting to a narrow trajectory distribution.

2) *Reward-Driven Curriculum Learning*: In the process of self-imitation generation, certain scenarios may be overly complex for the current policy. Trajectories generated in these scenarios are often suboptimal and can inject training noise that impairs stable policy convergence. Furthermore, it is crucial to prevent the model from overfitting to a narrow distribution of scenarios, which frequently leads to sub-optimal local minima.

To address these issues, we design a dynamic curriculum that prioritizes scenarios with high learning potential. For each scenario s_i , we assess its current learning potential using two metrics derived from sampled trajectories: the maximum trajectory reward $R_{\max}(s_i)$ and the reward range $R_{\text{range}}(s_i)$. A scenario is selected for training if it satisfies $R_{\max}(s_i) \geq \tau_{\max}$ and $R_{\text{range}}(s_i) \geq \tau_{\text{range}}$, where τ_{\max} guarantees learning feasibility, while τ_{range} promotes informative gradient variance to facilitate policy discrimination.

D. Efficient Inference of SIDP

Ascribed to our learning framework, SIDP generates concentrated and robust trajectory distributions. Consequently, it bypasses the conventional “generate-then-filter” paradigm that introduces non-negligible computational overhead during inference. Instead of relying on an auxiliary selector to filter multiple candidates, SIDP directly yields a viable trajectory through the denoising process, significantly streamlining the inference pipeline.

Another advantage is that SIDP enables the use of DDIM [13] for deterministic sampling. Compared to the stochastic DDPM [39], DDIM reduces actual inference steps significantly, thus further improving planning efficiency. To be clear, previous planners [1], [2] rely on sample stochasticity via DDPM to explore a broader range of trajectories, compensating for less refined policies.

IV. EXPERIMENTS

A. Evaluation Setup

1) *Benchmarks*: For comparative evaluation, we conducted experiments on the *InternVLA-N1 S1* benchmark [1] leveraging the high-fidelity Isaac Sim simulator. This benchmark

TABLE II: **Quantitative comparison on the InternVLA-N1 S1 benchmark.** We report Success Rate (SR, %) and Success weighted by Path Length (SPL, %) across different scene types and difficulty levels. mSR and mSPL denote the mean metrics averaged over all evaluated scenes.

Method	InternScenes				ClutteredEnv				mSR(↑)	mSPL(↑)		
	Commercial		Home		Easy		Hard					
	SR	SPL	SR	SPL	SR	SPL	SR	SPL				
iPlanner	53.02	51.44	39.16	37.27	89.80	88.70	80.69	79.28	59.14	57.57		
ViPlanner	64.43	62.90	43.61	42.07	82.08	81.98	67.24	67.07	60.90	59.83		
NavDP	71.25	68.89	57.38	55.08	93.37	91.44	88.71	86.31	73.22	70.95		
SIDP (Ours)	81.19	73.36	63.17	56.48	94.36	89.86	91.58	86.78	79.11	72.72		

focuses on closed-loop sequential navigation (real-time), requiring the agent to reach goals through continuous, multi-step navigation. The benchmark comprises 60 diverse scenes, including 40 from *InternScenes* (equally divided into home and commercial) and 20 from *ClutteredEnv* (including 10 easy and 10 hard). For each scene, 100 start-goal pairs were randomly sampled in unoccupied spaces. Initial orientations were pre-calculated via path planning to ensure collision-free initialization.

For the ablation studies, we curated a compact yet representative benchmark derived from the *InternData-N1* dataset [1], encompassing 5 scenes and 500 total trials. In contrast to the real-time interaction of the *InternVLA-N1 S1* benchmark, this setup focuses on one-shot trajectory generation (single-step), evaluating the policy’s ability to plan an entire path in a single inference. To ensure evaluation consistency, we utilized fixed starting positions paired with randomly sampled goals for each scene.

2) *Evaluation Metrics*: To facilitate a comprehensive and rigorous evaluation, we report the following standard metrics for the main navigation task:

- **Success Rate (SR, %):** The percentage of episodes where the agent successfully reaches within 0.5 m of the target.
- **Success weighted by Path Length (SPL, %):** A metric evaluating both success and path efficiency, defined as:

$$\text{SPL} = \frac{1}{N} \sum_{i=1}^N S_i \cdot \frac{L_i}{\max(P_i, L_i)}, \quad (9)$$

where S_i is the binary success indicator, L_i is the geodesic shortest path length, and P_i is the actual path length taken by the agent.

Furthermore, to analyze safety and exploration quality in the ablation studies on our custom benchmark, we introduce three additional metrics:

- **Collision Rate (CR, %):** The proportion of episodes in which the agent encounters at least one collision, serving as a key indicator of navigation safety.
- **Distance To Goal (DTG, m):** The average Euclidean distance between the agent’s final position and the goal.
- **Exploration Area (EA, m²):** The non-redundant union of 16 sampled trajectories (each modeled as a 0.2m-wide swept area), quantifying goal-agnostic exploration diversity.

B. Implementation Details

1) *Training Scenario Construction*: To facilitate efficient self-imitation learning without the computational overhead of full physics simulation, we construct an interactive environment based on the *InternData-N1* dataset [1].

Specifically, we sample the agent’s initial poses from the expert trajectories provided in the dataset, employing temporal subsampling to enhance state diversity. Subsequently, point goals of varying difficulty are generated using the scene’s global Euclidean Signed Distance Field (ESDF), which also ensures collision-free initialization. Furthermore, collision detection is approximated by directly querying ESDF values along predicted paths, enabling the agent to rapidly evaluate trajectory safety against complex scene geometries during the iterative training process. The detailed reward formulation is presented in Tab. I.

2) *Network Architecture and Training Details*: We utilize the diffusion-based network, NavDP [1], as the initialization for our policy network, while omitting the auxiliary critic network typically required for trajectory selection.

The model is optimized using the AdamW optimizer with a learning rate of 2×10^{-5} . We employ an effective batch size of 128 (64×2), distributed across two NVIDIA A100 GPUs. The entire training process spans approximately 35 hours.

C. Comparisons with State-of-the-art Methods

We compare our method with several learning-based visual navigation approaches on key metrics of success and efficiency. ViPlanner and iPlanner are planning-based baselines that rely on learned perception modules coupled with analytical planners. NavDP shares a similar diffusion-based architecture to ours but is trained purely via imitation learning without self-imitation, serving as our primary baseline for assessing both robustness and efficiency.

1) *Navigation Performance Analysis*.: Quantitative results are summarized in Table II. Our proposed SIDP achieves the highest SR across all evaluated scenarios and demonstrates superior overall performance in SPL, as evidenced by the highest mean metrics (mSR and mSPL). Notably, the performance advantage of SIDP is most pronounced in the challenging *InternScenes* environments. In the *Commercial* and *Home* scenarios, which feature intricate furniture layouts and narrow traversable regions, SIDP outperforms NavDP by substantial margins of 9.94% and 5.79% in Success Rate, respectively. This demonstrates that the self-imitation mechanism effectively refines the diffusion policy, enabling it to

TABLE III: Inference time comparison between different models and scheduler.

Method	Scheduler	Denoising Steps	Time (ms)	SR(\uparrow)
NavDP	DDPM	10	273 (1 \times)	0.549
SIDP	DDPM	10	132 (2.07 \times)	0.670
SIDP	DDIM	10	131 (2.08 \times)	0.670
SIDP	DDIM	5	110 (2.48 \times)	0.674
SIDP	DDIM	3	99 (2.76 \times)	0.655

handle complex geometric constraints where imitation learning often struggles.

In the randomized *ClutteredEnv* environments, the performance gap between SIDP and NavDP narrows. We attribute this to a performance saturation effect: the baseline NavDP is already highly competent in these simpler obstacle avoidance tasks (achieving $> 93\%$ SR in Easy settings). However, even in these scenarios, SIDP maintains a consistent edge, validating its generalizability and robustness.

2) *Computational Efficiency*.: Beyond success rates, we evaluate the efficiency of our approach for real-world deployment. We measure the path inference latency against NavDP on an NVIDIA Jetson Orin Nano Super development kit (8GB RAM), a representative hardware configuration for modern mobile robots. As shown in Table III, over 100 trials on this device, SIDP with 10-step DDPM sampling achieved an average inference time of 132 ms, nearly 2 \times faster than NavDP(273 ms).

Utilizing DDIM sampling further optimizes the inference pipeline. Notably, when reducing the denoising steps to 5, the inference time decreases to 110ms while the SR even marginally improves to 0.674. Even with a highly compressed 3-step configuration, SIDP maintains a competitive SR of 0.655 with a latency of only 99ms. These results identify the 5-step DDIM configuration as the optimal balance, providing the highest success rate with significant computational efficiency.

This efficiency gain stems from our self-imitation framework, which generates a concentrated and reliable trajectory distribution, eliminating the need for stochastic and computationally expensive trajectory sampling and filtering seen in traditional diffusion planners.

D. Ablation Studies and Analysis

To evaluate the contribution of each key component in our framework, we conduct a series of ablation experiments corresponding to the strategies introduced in Section III: (1) the impact of the proposed **Reward-Guided Self-Imitation** mechanism (Section III-B) on training stability and convergence; (2) the influence of the **Goal-agnostic Exploration** strategy (Section III-C) designed to diversify the training data; and (3) the effectiveness of the **Reward-Driven Curriculum Learning** scheme(Section III-C) in prioritizing high-reward training scenarios.

1) *Reward-Guided Self-Imitation*: To validate the advantage of our exponential weighting strategy, we compare it with another linear weighting baseline, denoted as *Lin. Weig*, where importance weights are assigned linearly based on the reward for all positive trajectories, instead of using the Softmax transformation. As illustrated in Figs. 3 and 4, Lin.

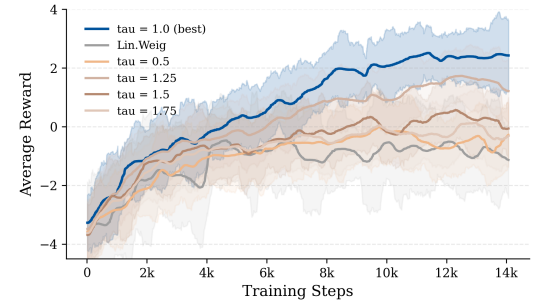


Fig. 3: Learning curves of SIDP under different temperature coefficients during training. The curves are smoothed using a Gaussian filter ($\sigma = 10$), and the shaded region indicates the rolling-window standard deviation, capturing performance fluctuations caused by environment variations and randomly sampled navigation goals.

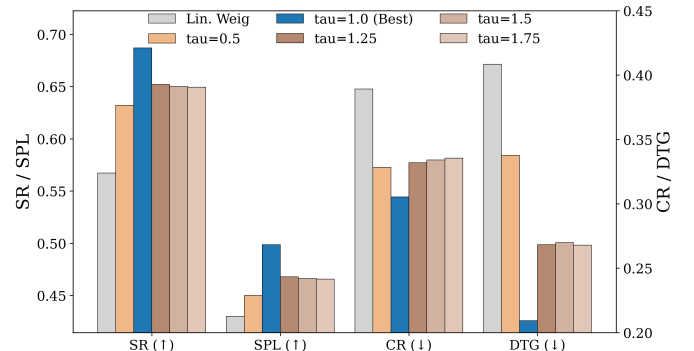


Fig. 4: Ablation study of the reward-guided self-imitation mechanism and the Softmax temperature coefficient τ .

Weig lags far behind the exponential function with $\tau = 1.0$ in overall performance, which may be caused by its lack of sufficient selection pressure to distinguish trajectories.

We also investigate the temperature coefficient τ , which modulates this selection sharpness. In Figs. 3 and 4, $\tau = 1.0$ yields optimal performance. Extreme values prove detrimental: low τ leads to instability by over-fitting to a few samples, while high τ flattens the action importance distribution.

2) *Goal-agnostic Exploration*: To evaluate the impact of goal-agnostic trajectory augmentation on the point-goal navigation and goal-agnostic exploration, we compare models trained with and without *goal-agnostic* setting. Note that in the goal-agnostic exploration, no explicit target is provided thus only the CR and EA metrics are reported.

As shown in Fig 5, in the point-goal navigation tasks, incorporating the goal-agnostic trajectory augmentation during training leads to trajectories that are both safer and closer to the target, suggesting that goal-agnostic trajectory augmentation acts as a form of regularization that improves the overall navigation performance. In the goal-agnostic exploration tasks, the model trained with goal-agnostic settings achieves a lower CR and a higher EA, indicating its ability to generate safe and diverse trajectories for exploration. Notably, this suggests that the goal-agnostic setting enables the model to produce consistently high-quality trajectories while preserving the inherent multi-modal distribution characteristic of diffusion policies.

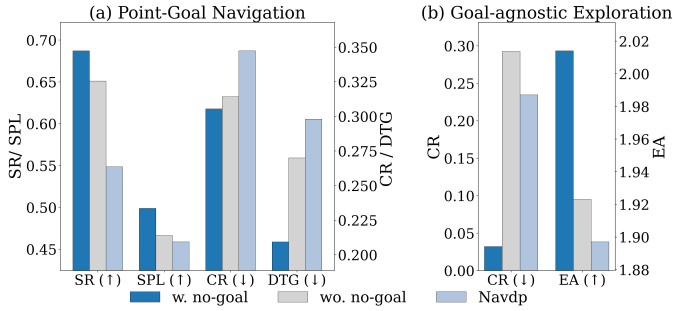


Fig. 5: Ablation study of goal-agnostic training under different evaluation settings.

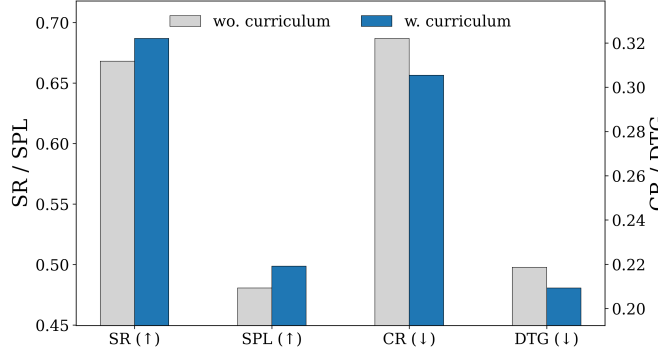


Fig. 6: Ablation study of reward-driven curriculum learning on policy performance.

3) *Reward-Driven Curriculum Learning*: We investigate the effect of the reward-driven curriculum learning. As shown in Fig. 6, the policy trained with curriculum learning achieves higher SR, SPL and lower CR, DTG. The improved SR and reduced CR suggest that the policy benefits from prioritizing feasible scenarios as governed by R_{\max} , thereby mitigating the destabilizing influence of failed trajectories. Simultaneously, the gains in SPL and DTG align with our objective of leveraging R_{range} to provide discriminative signals, which encourages the model to optimize for navigational efficiency rather than mere task completion.

E. Real-world Deployment

Fig. 7 demonstrates the robust real-world performance of our method on Unitree Go2 and Agilex T-rex platforms. We utilize a stereo camera setup to acquire synchronized left and right RGB images, which are subsequently processed by BANet [40] to estimate the corresponding high-density depth maps.

Our SIDP framework processes RGB-D inputs alongside human-specified goal points, enabling empirical validation across diverse environments such as offices and hallways. The time-lapse trajectory (bottom right) demonstrates a continuous, collision-free path, highlighting the sim-to-real adaptability and stable navigation of our framework in complex scenes.

V. CONCLUSION

We introduced the Self-Imitated Diffusion Policy (SIDP) framework, which combines self-imitation learning with diffusion models to enable efficient and robust path planning

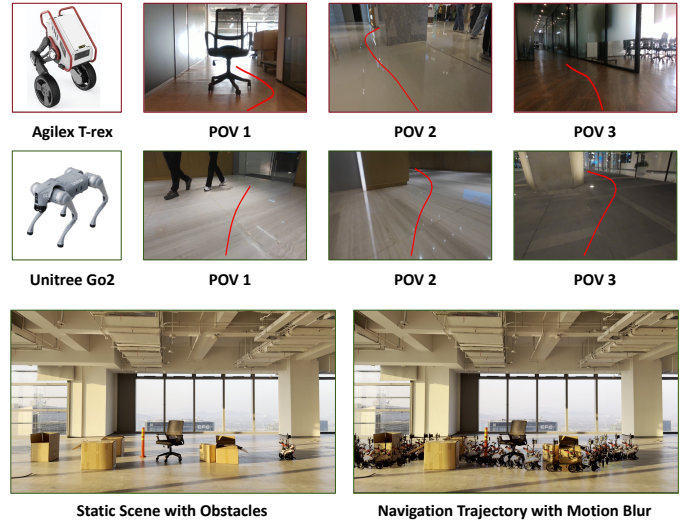


Fig. 7: **Qualitative results of visual end-to-end navigation.** Top: Diverse robot platforms (wheeled and quadruped) and their respective POV trajectories. Bottom: Third-person perspective of a navigation trial, showing the static environment (left) and the generated collision-free trajectory (right) visualized via motion blur.

for visual navigation. By continuously learning from self-generated experiences, SIDP overcomes the suboptimal and incomplete nature of expert datasets, training policies that generate higher-performing trajectories, which also reduces the need for complex trajectory selection, lowering computational overhead and improving efficiency. The framework also incorporates two key strategies: goal-agnostic exploration to enhance regularization, and reward-driven curriculum learning to enhance data utility, further optimizing the policy’s performance. Experimental results demonstrate that SIDP outperforms existing methods across various metrics, including success rates(SR), success weighted by path Length(SPL). Additionally, SIDP achieves a $2.5\times$ speedup in inference latency on embedded platforms, proving its suitability for real-time robotic deployment.

In conclusion, SIDP provides a robust and efficient solution for visual navigation, bridging the gap between generative models and practical robotic applications.

ACKNOWLEDGMENT

This research was supported by the Key Scientific Research Program of Hangzhou Municipal Bureau of Science and Technology grants 2025SZD1A01.

REFERENCES

- [1] W. Cai, J. Peng, Y. Yang, Y. Zhang, M. Wei, H. Wang, Y. Chen, T. Wang, and J. Pang, “NavDP: Learning sim-to-real navigation diffusion policy with privileged information guidance.” [Online]. Available: <http://arxiv.org/abs/2505.08712>
- [2] A. Sridhar, D. Shah, C. Glossop, and S. Levine, “NoMaD: Goal masked diffusion policies for navigation and exploration,” in *2024 IEEE International Conference on Robotics and Automation (ICRA)*. IEEE, pp. 63–70. [Online]. Available: <https://ieeexplore.ieee.org/document/10610665/>

[3] M. Janner, Y. Du, J. B. Tenenbaum, and S. Levine, “Planning with diffusion for flexible behavior synthesis.” [Online]. Available: <http://arxiv.org/abs/2205.09991>

[4] A. Popov, A. Degirmenci, D. Wehr, S. Hegde, R. Oldja, A. Kamenev, B. Douillard, D. Nistér, U. Müller, R. Bhargava, S. Birchfield, and N. Smolyanskiy, “Mitigating Covariate Shift in Imitation Learning for Autonomous Vehicles Using Latent Space Generative World Models,” May 2025, arXiv:2409.16663 [cs]. [Online]. Available: <http://arxiv.org/abs/2409.16663>

[5] H. Shi, X. Deng, Z. Li, G. Chen, Y. Wang, and L. Nie, “DAgger diffusion navigation: DAgger boosted diffusion policy for vision-language navigation,” version: 1. [Online]. Available: <http://arxiv.org/abs/2508.09444>

[6] Y. Zeng, H. Ren, S. Wang, J. Huang, and H. Cheng, “NaviDiffusor: Cost-guided diffusion model for visual navigation.” [Online]. Available: <http://arxiv.org/abs/2504.10003>

[7] A. Bar, G. Zhou, D. Tran, T. Darrell, and Y. LeCun, “Navigation world models,” in *Proceedings of the Computer Vision and Pattern Recognition Conference*, 2025, pp. 15 791–15 801.

[8] Z. Li, W. Yao, Z. Wang, X. Sun, J. Chen, N. Chang, M. Shen, Z. Wu, S. Lan, and J. M. Alvarez, “Generalized trajectory scoring for end-to-end multimodal planning.” [Online]. Available: <http://arxiv.org/abs/2506.06664>

[9] J. Oh, Y. Guo, S. Singh, and H. Lee, “Self-Imitation Learning,” June 2018, arXiv:1806.05635 [cs]. [Online]. Available: <http://arxiv.org/abs/1806.05635>

[10] Z. Wang, J. J. Hunt, and M. Zhou, “Diffusion policies as an expressive policy class for offline reinforcement learning,” *arXiv preprint arXiv:2208.06193*, 2022.

[11] A. Z. Ren, J. Lidard, L. L. Ankile, A. Simeonov, P. Agrawal, A. Majumdar, B. Burchfiel, H. Dai, and M. Simchowitz, “Diffusion policy policy optimization,” *arXiv preprint arXiv:2409.00588*, 2024.

[12] N. Yang, J. Gao, F. Gao, Y. Wu, and C. Yu, “Fine-tuning diffusion policies with backpropagation through diffusion timesteps,” 2025. [Online]. Available: <https://arxiv.org/abs/2505.10482>

[13] J. Song, C. Meng, and S. Ermon, “Denoising diffusion implicit models,” *arXiv preprint arXiv:2010.02502*, 2020.

[14] R. Mur-Artal and J. D. Tardos, “ORB-SLAM2: an open-source SLAM system for monocular, stereo and RGB-d cameras,” vol. 33, no. 5, pp. 1255–1262. [Online]. Available: <http://arxiv.org/abs/1610.06475>

[15] C. Campos, R. Elvira, J. J. G. Rodríguez, J. M. M. Montiel, and J. D. Tardós, “ORB-SLAM3: An accurate open-source library for visual, visual-inertial and multi-map SLAM,” vol. 37, no. 6, pp. 1874–1890. [Online]. Available: <http://arxiv.org/abs/2007.11898>

[16] E. Wijmans, A. Kadian, A. Morcos, S. Lee, I. Essa, D. Parikh, M. Savva, and D. Batra, “DD-PPO: Learning near-perfect PointGoal navigators from 2.5 billion frames.” [Online]. Available: <http://arxiv.org/abs/1911.00357>

[17] J. Ye, D. Batra, E. Wijmans, and A. Das, “Auxiliary tasks speed up learning PointGoal navigation.” [Online]. Available: <http://arxiv.org/abs/2007.04561>

[18] S. S. Desai and S. Lee, “Auxiliary tasks for efficient learning of point-goal navigation,” in *2021 IEEE Winter Conference on Applications of Computer Vision (WACV)*. IEEE, pp. 717–725. [Online]. Available: <https://ieeexplore.ieee.org/document/9423043/>

[19] P. Anderson, Q. Wu, D. Teney, J. Bruce, M. Johnson, N. Sünderhauf, I. Reid, S. Gould, and A. v. d. Hengel, “Vision-and-language navigation: Interpreting visually-grounded navigation instructions in real environments.” [Online]. Available: <http://arxiv.org/abs/1711.07280>

[20] D. Fried, R. Hu, V. Cirik, A. Rohrbach, J. Andreas, L.-P. Morency, T. Berg-Kirkpatrick, K. Saenko, D. Klein, and T. Darrell, “Speaker-follower models for vision-and-language navigation.” [Online]. Available: <http://arxiv.org/abs/1806.02724>

[21] D. Shah, B. Eysenbach, G. Kahn, N. Rhinehart, and S. Levine, “ViNG: Learning open-world navigation with visual goals,” in *2021 IEEE International Conference on Robotics and Automation (ICRA)*, pp. 13 215–13 222. [Online]. Available: <http://arxiv.org/abs/2012.09812>

[22] J. Krantz, A. Gokaslan, D. Batra, S. Lee, and O. Maksymets, “Waypoint models for instruction-guided navigation in continuous environments.” [Online]. Available: <http://arxiv.org/abs/2110.02207>

[23] Y. Li, J. Song, and S. Ermon, “InfoGAIL: Interpretable imitation learning from visual demonstrations.” [Online]. Available: <http://arxiv.org/abs/1703.08840>

[24] Q. Wu, X. Gong, K. Xu, D. Manocha, J. Dong, and J. Wang, “Towards target-driven visual navigation in indoor scenes via generative imitation learning.” [Online]. Available: <http://arxiv.org/abs/2009.14509>

[25] S. Ross, G. Gordon, and D. Bagnell, “A reduction of imitation learning and structured prediction to no-regret online learning,” in *Proceedings of the Fourteenth International Conference on Artificial Intelligence and Statistics*. JMLR Workshop and Conference Proceedings, pp. 627–635, ISSN: 1938-7228. [Online]. Available: <https://proceedings.mlr.press/v15/ross11a.html>

[26] K. Kim, K. Shin, M. W. Lee, M. Lee, M. Lee, and B.-T. Zhang, “Visual hindsight self-imitation learning for interactive navigation,” vol. 12, pp. 83 796–83 809. [Online]. Available: <http://arxiv.org/abs/2312.03446>

[27] A. Ajay, Y. Du, A. Gupta, J. Tenenbaum, T. Jaakkola, and P. Agrawal, “Is conditional generative modeling all you need for decision-making?” [Online]. Available: <http://arxiv.org/abs/2211.15657>

[28] Z. Liang, Y. Mu, H. Ma, M. Tomizuka, M. Ding, and P. Luo, “SkillDiffuser: Interpretable hierarchical planning via skill abstractions in diffusion-based task execution.” [Online]. Available: <http://arxiv.org/abs/2312.11598>

[29] Y. Luo, U. A. Mishra, Y. Du, and D. Xu, “Generative trajectory stitching through diffusion composition.” [Online]. Available: <http://arxiv.org/abs/2503.05153>

[30] J. Carvalho, A. T. Le, M. Baierl, D. Koert, and J. Peters, “Motion planning diffusion: Learning and planning of robot motions with diffusion models.” [Online]. Available: <http://arxiv.org/abs/2308.01557>

[31] W. Yu, J. Peng, H. Yang, J. Zhang, Y. Duan, J. Ji, and Y. Zhang, “LDP: A local diffusion planner for efficient robot navigation and collision avoidance,” in *2024 IEEE/RSJ International Conference on Intelligent Robots and Systems (IROS)*, pp. 5466–5472, ISSN: 2153-0866. [Online]. Available: <https://ieeexplore.ieee.org/document/10802009/>

[32] H. Ren, Y. Zeng, Z. Bi, Z. Wan, J. Huang, and H. Cheng, “Prior does matter: Visual navigation via denoising diffusion bridge models.” [Online]. Available: <http://arxiv.org/abs/2504.10041>

[33] B. Liao, S. Chen, H. Yin, B. Jiang, C. Wang, S. Yan, X. Zhang, X. Li, Y. Zhang, Q. Zhang, and X. Wang, “DiffusionDrive: Truncated diffusion model for end-to-end autonomous driving.” [Online]. Available: <http://arxiv.org/abs/2411.15139>

[34] B. Yang, H. Su, N. Gkanatsios, T.-W. Ke, A. Jain, J. Schneider, and K. Fragkiadaki, “Diffusion-ES: Gradient-free planning with diffusion for autonomous driving and zero-shot instruction following.” [Online]. Available: <http://arxiv.org/abs/2402.06559>

[35] Y. Zheng, R. Liang, K. Zheng, J. Zheng, L. Mao, J. Li, W. Gu, R. Ai, S. E. Li, X. Zhan, and J. Liu, “Diffusion-based planning for autonomous driving with flexible guidance.” [Online]. Available: <http://arxiv.org/abs/2501.15564>

[36] K. Kondo, A. Tagliabue, X. Cai, C. Tewari, O. Garcia, M. Espitia-Alvarez, and J. P. How, “CGD: Constraint-guided diffusion policies for UAV trajectory planning.” [Online]. Available: <http://arxiv.org/abs/2405.01758>

[37] J. Peters, K. Mulling, and Y. Altun, “Relative entropy policy search,” in *Proceedings of the AAAI Conference on Artificial Intelligence*, vol. 24, no. 1, 2010, pp. 1607–1612.

[38] A. B. Owen, *Monte Carlo theory, methods and examples*. Stanford University, 2013, available online at <https://statweb.stanford.edu/~owen/mc/>.

[39] J. Ho, A. Jain, and P. Abbeel, “Denoising diffusion probabilistic models,” *Advances in neural information processing systems*, vol. 33, pp. 6840–6851, 2020.

[40] F.-J. Tsai, Y.-T. Peng, C.-C. Tsai, Y.-Y. Lin, and C.-W. Lin, “Banet: A blur-aware attention network for dynamic scene deblurring,” *IEEE Transactions on Image Processing*, vol. 31, pp. 6789–6799, 2022.